Appl. Phys. B 26, 43–48 (1981)

Applied Physics

Operating Characteristics of UV and IR Hollow-Cathode Silver, Gold and Copper Ion Lasers*

K. Jain

IBM Research Laboratory, San Jose, CA 95193, USA

S. A. Newton**

Edward L. Ginzton Laboratory, Stanford University, Stanford, CA 94305, USA

Received 2 March 1981/Accepted 10 April 1981

Abstract. Operating characteristics of silver, gold and copper vapor hollow-cathode lasers are presented. Dependence of the output power, gain and threshold current on the cathode length, composition of the buffer gas, and mirror transmission is described. Studies of multicomponent hollow cathodes which produce laser lines of several elements simultaneously are also presented.

PACS: 42.55. Hq, 34.70.+*e*, 42.60. By

Recently, there have been several studies of singly-ionized and neutral metal vapor lasers employing the hollow-cathode discharge [1–13]. Laser action has been obtained in a large number of metals, and the observed transitions now cover a wide range from ultraviolet to infrared. CW output powers of 1 W in the near ir [7c] and 1 mW in the deep uv [10c] have been reported. In this paper we describe various operating characteristics of Cu, Ag and Au vapor lasers in the uv and ir. In particular, we present out studies of the dependence of the output power, gain and threshold current on the cathode length, pressure and composition of the buffer gas, and the output mirror transmission. We also describe operation of several multicomponent hollow cathodes which produce laser transitions from several elements simultaneously.

1. Ag: He Laser at 224 nm

The $5d^1S_0 \rightarrow 5p^1P_1^0$ transition in AgII at 224.3 nm is excited by resonant charge-transfer collisions between ground state Ag atoms and He ions:

$$\mathrm{He}^+(^2S_{1/2}) + \mathrm{Ag}(^2S_{1/2}) \rightarrow \mathrm{He}(^1S_0) + \mathrm{Ag}^+(5d^1S_0) + 0.34\,\mathrm{eV}. \quad (1)$$

It is the shortest wavelength cw laser transition known to date, first observed by McNeil et al. [7b]. We have previously reported a threshold of 2A, a cw output power of 1.46 mW, and a pulsed output power of 50 mW for this line [10c]. Here we describe our results on the measurement of gain for this transition. The hollow cathode was a 25 cm long rectangular slot, and the other experimental details were as reported previously [10c, a]. The gain was calculated by measuring the output power at a fixed discharge current for various output mirror couplings. At a pulsed input current of 40 A, the peak output power for measured mirror transmissions of 0.14, 1.15, 1.85, and 2.9% was 6.8, 24, 50.1 and 51.5 mW, respectively. Since the line broadening is expected to be homogeneous [14], we used the expression [15]

$$P = \frac{T}{S}\left(\frac{G}{A+T} - 1\right) \quad (2)$$

to calculate the gain. Here, P is the output power, T the mirror transmission, A the total cavity loss, G the unsaturated gain, and S is a saturation parameter

* Part of this work was done while the authors were at Hewlett-Packard Laboratories, Palo Alto, CA 94304, USA

** On leave of absence from Hewlett-Packard Laboratories, Palo Alto, CA 94304, USA

0340-3793/81/0026/0043/$01.20

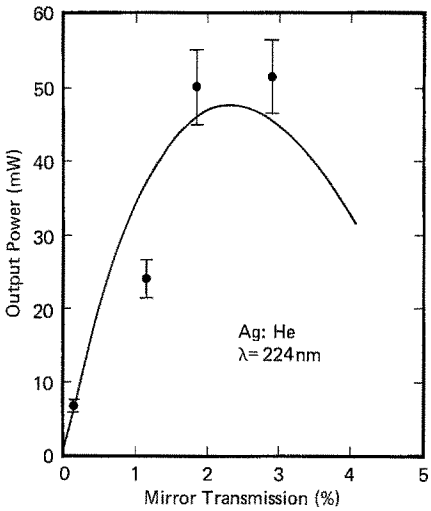

Fig. 1. Dependence of the output power on the mirror transmission for the 224 nm line from an Ag: He hollow-cathode laser. The solid curve is drawn from (2) with $G=25\%/\text{m}$, $1/S=6$ W and $A=0.07$

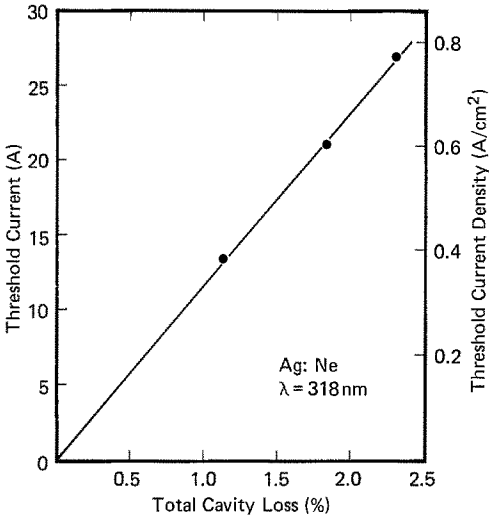

Fig. 2. Dependence of the threshold current on the total cavity loss (mirror transmission + absorption) for the 318 nm line from an Ag:Ne hollow-cathode laser

equal to inverse of the power (in the cavity) at which the gain falls to half its unsaturated value. As the mirror absorption was also unknown, it was determined from the power vs. transmission measurements. From the four (T,P) pairs of data, a best fit determination gave $G=25\%/\text{m}$, $1/S=6$ watts and $A=7\%$. The curve obtained by using these values in (2) is shown in Fig. 1 along with the experimental points. It is seen that the optimum output coupling for this laser with a 25 cm long cathode, given by

$$T_{\text{opt}}=\sqrt{GA}-A, \tag{3}$$

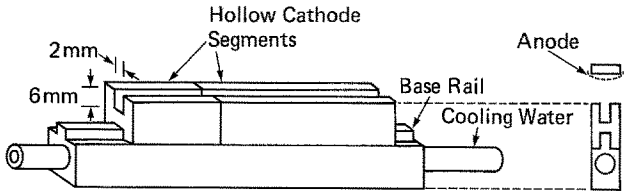

Fig. 3. Segmented slot hollow cathode. The total hollow cathode length is varied by placing segments of various lengths on the base rail

is 2.35%. Using (2), one can also estimate the power obtainable from longer cathodes if the current density is maintained the same. Thus, for a 1 m long cathode with a discharge current of 160 A, the total gain G becomes 0.5, and (3) gives $T_{\text{opt}}=11.7\%$. This can be used in (2) to obtain $P=1.18$ W.

2. Ag: Ne Laser at 318 nm

This transition in AgII, $5s^2\,{}^1G_4\rightarrow 5p^3F_3^0$, is excited by charge transfer collisions with Ne^+. It is much weaker than the 224 nm line and has a much higher threshold. The threshold currents for a cathode of the same length as before for three different mirror pairs are plotted in Fig. 2. Since at threshold the cavity loss equals the unsaturated gain, Fig. 2 also shows how the gain varies with the current density. The linear dependence of threshold on the total cavity loss indicates that the optimum metal vapor density is obtained at much higher currents. The power output for the three mirror transmissions of 0.16, 0.86, and 1.9% was 45, 50, and 28 mW, respectively, at a pulsed input current of 50 A. Using these values and (2), the best-fit values of the gain and the inverse saturation parameter were found to be 5%/m and 21 W, respectively. Thus, the 224 nm line of AgII is superior to its 318 nm line in every respect except degradation of the high-reflectivity dielectric mirrors, which was found to be much more severe at the former wavelength.

3. Au: He Laser in the UV

For an Au: He discharge lasing at the 282 nm AuII transition originating from the $7s^1D_2$ level, we studied the dependence of the output power and threshold current on the cathode length. The hollow cathode was a 2 mm × 6 mm slot in cross section and its length was varied by placing segments of various lengths on a 25 cm long rail (Fig. 3). All the segments and the rail were made of copper and then gold plated. Since the current density in the hollow cathode slot is very much larger than on the outer parts of the cathode, the

contribution of the unused rail where there is no segment is negligible. The anode was made of a perforated stainless steel sheet and its length was kept fixed at 25 cm. The buffer gas was a 100:1 mixture of He and Ar at a total pressure of 22 Torr. True cw lasing was obtained at cathode lengths down to 5 cm. With a cathode length of 2.5 cm [16] the lasing was quasi-cw with current pulses of 300 μs duration at a repetition rate of 33 Hz. The output mirror transmission was 0.1 %. In Fig. 4 we show the output power and threshold current measured for various cathode lengths. All power outputs shown in Fig. 4 are peak values obtained with 10 A current pulses. Note that for a given discharge current, the current *density* is higher in a shorter cathode. It is seen that whereas the output power increases monotonically with the cathode length, the threshold current shows a minimum. The slight increase in the threshold current for lengths longer than 10–15 cm is perhaps due to the fact that with a lower current *density*, the cathode fall voltage is lower, which results in a lower gold density through a diminished sputtering yield and thus poorer gain. The rapid increase in the threshold current with shorter lengths is more difficult to understand, but a probable explanation may be the depopulation of the upper laser level by superelastic collisions with slow electrons which become more abundant as the current density increases. Similar behavior for several transitions in the CuII laser was observed by McNeil [17]. This argument is better understood if one replots the threshold data of Fig. 4 in the form of gain per unit length vs. cathode current density. Since the cavity loss was the same for all data points in Fig. 4, inverse of the cathode length is proportional to the gain per unit length at the corresponding threshold current density. This is plotted in Fig. 5. It is at once seen that the increase in gain per unit cathode length becomes less and less as the cathode current density increases.

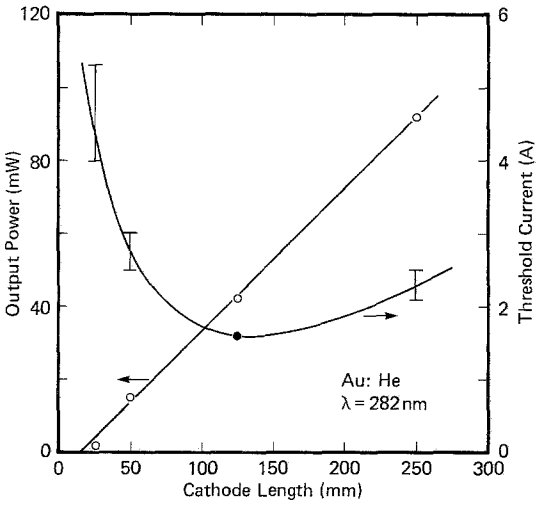

Fig. 4. Dependence of the output power and threshold current of the 282 nm AuII line on the length of the hollow cathode. The output power was measured at a discharge current of 10 A

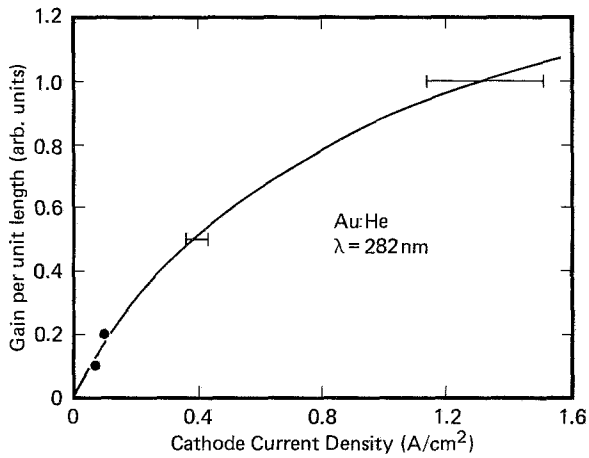

Fig. 5. The data of Fig. 4 replotted to display the variation of the gain per unit length vs. the cathode current density for the 282 nm AuII transition

4. Cu: Ne Laser in the UV

Several hollow-cathode designs were investigated for the Cu:Ne system lasing in the 250 nm region. In addition to the slot geometry shown in Fig. 3, the structures shown in Fig. 6 were also used with different cathode lengths. The cylindrical mesh anode which surrounds the entire cathode, as shown in Fig. 6a, was found to produce the most stable discharge of all the anode designs attempted by us. Instead of a mesh, when a more rugged solid stainless steel tube was used (Fig. 6c) as an anode, the discharge stability became inferior – arcing was observed at dc currents higher than 4 A, although pulsed operation was satisfactory at $I > 30$ A. Figure 6b shows a "flute" cathode. The optimum hollow-cathode i.d. was found to be 5 mm.

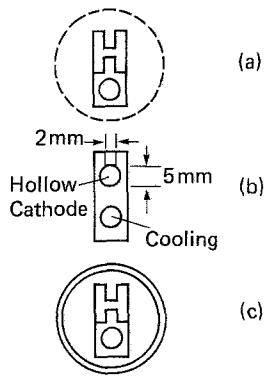

Fig. 6a–c. Various anode-cathode structures: (a) slotted and segmented hollow cathode with a circular mesh anode; (b) a flute cathode; (c) same as (a), except with a solid tubular anode

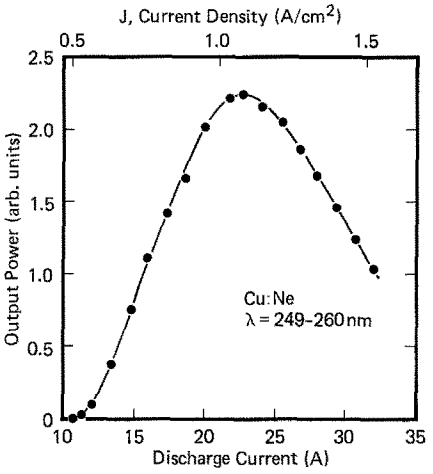

Fig. 7. Dependence of the output power on the discharge current for a Cu:Ne laser in the 250 nm region. The cathode was 15 cm long and the buffer gas also contained a slight amount of xenon

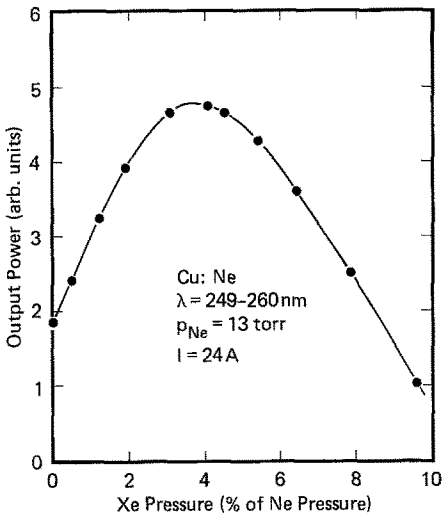

Fig. 8. Optimization of the xenon pressure at a constant current in the Cu:Ne laser

2 mm diameter holes for discharge paths to the anode were provided on the top at intervals of 25 mm. This is the geometry that produced the highest output power: at a peak input current of 40 A, pulse width of 40 μs and repetition rate of 250 Hz, a multiline power output of 800 mW was measured from a 25 cm long cathode, with a 0.23:0.11:0.37:0.29 distribution in the 2486, 2529, 2591, and 2599–2600 Å lines.

The dependence of the output power on discharge current is shown in Fig. 7. These data were taken on a 15 cm long slot cathode with a cylindrical mesh anode and a rare gas mixture of 13 Torr of neon and 0.47 Torr of xenon. Previously, several properties of a Cu:Ne hollow cathode discharge have been measured by de Hoog et al. [18] at low current densities. These authors found that, except for an initial threshold-like behavior, both the copper atom density and the spontaneous emission from the 2600 Å laser transition increased linearly with current for current densities, J, up to $\sim 0.5\ \mathrm{A/cm^2}$. A unified discharge-sputtering theory developed by Warner et al. [19], which takes into account the sputtering action of both the buffer-gas ions and the metal ions, explains the above observations of De Hoog et al. [18] extremely well. Since for charge-transfer-excited transitions the laser output should vary as the product of the ground-state neon-ion density and the ground-state neutral copper density, and since the neon-ion density saturates at high current densities, a linear increase in the laser output is expected with the discharge current. Our data (Fig. 7) show that this linear dependence continues to $J \simeq 1\ \mathrm{A/cm^2}$. It shows a maximum at $J \sim 1.1\ \mathrm{A/cm^2}$ and then begins to decline. There are several reasons for this behavior. At low current densities, the dominant ion in the discharge is Ne^+. However, since the ionization potential of Cu (7.72 eV) is significantly lower than that of Ne (21.56 eV), it becomes more difficult to maintain the Ne^+ density as the current, and hence the Cu density, increases. Consequently, an optimum is reached, and for higher currents the Ne^+ population goes down, resulting in lower laser output. Another possible mechanism is de-excitation of the upper laser levels by slow-electron collisions. It is also likely that at high current densities direct electron excitation of the lower laser state takes place from the 4s or the ion ground state [11c]. A fourth possible mechanism for the decline of the laser power at higher currents is radiation trapping. However, estimates [17] show that radiation trapping effects should become significant only at output power levels much higher than the 20 mW obtained from the present 15 cm long cathode.

The existence of an optimum metal vapor density *at a constant discharge current* is demonstrated by introducing a small amount of xenon into the discharge and varying its partial pressure. Figure 8 shows the results. It is seen that at a discharge current of 24 A, the output reaches its optimum value at a neon-xenon ratio of 100:4. Figure 8 also suggests an interesting application of the addition of a heavier rare gas to the discharge. Since the cathodic sputtering yield by Xe ions is several times larger than by Ne ions for most metals [20], at low currents densities most of the metal vapor can be produced by Xe, and thus the discharge current can be varied *independently* keeping the metal vapor density fixed near its optimum value. It will be recognized that without the heavy buffer gas, such independent control would not be possible.

Similar results were also obtained when the argon pressure was varied in an Ag:He discharge lasing in

the ir at 840 nm. For a constant current of 5 A and constant He pressure of 15 Torr, the variation in the output power from a 25 cm long cathode is shown in Fig. 9, indicating an optimum near $p(\mathrm{Ar}) \sim 1\%$ of $p(\mathrm{He})$. Here, as in the Cu:Ne+Xe case, the output initially rises because a higher Ar pressure produces more Ag atoms by sputtering; at very high Ar pressures the trend reverses because with increased density of low ionization potential Ag and Ar atoms, it becomes more difficult to ionize He.

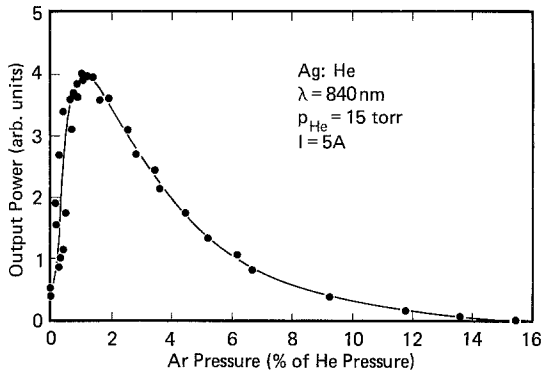

Fig. 9. Optimization of the partial pressure of argon in Ag:He infrared laser. The current was kept constant at 5 A

5. Multi-Component Hollow-Cathode Lasers

In addition to cw oscillation, low threshold, low noise and compact construction, a major advantage of metal ion lasers is the simultaneous availability of a large number of lasing transitions. Thus, with more than one metal in the discharge, one should be able to invert a signficantly larger number of lines. With a view to explore this, we investigated several multicomponent hollow-cathode systems. In the simplest version of the multicomponent laser, hollow-cathode segments of Cu, Ag, and Au of various lengths were placed on a copper rail, as in Fig. 6a, and simultaneous lasing was observed at several lines from all three metals. For example, with Ag, Cu, and Au segments of lengths 25, 50, and 205 mm, respectively, a total of 10 transitions was observed at a discharge current of 16 A: 5 from Ag^+ (801, 825, 832, 838, and 840 nm), 2 from Cu^+ (781 and 783 nm), and 3 from Au^+ (760, 827, and 860 nm). Evidently, by proper choice of the cathode composition, the number of lines and the distribution of the total output among them can be optimized.

A second approach for a multicomponent laser was demonstrated by using an alloy cathode. With an He–Ar discharge excited in a 280 mm long hollow cathode made of brass (61.5% Cu+35.5% Zn+3% impurities), oscillation was seen at 13 lines at an input current of 25 A: 2 from Zn^+ (748 and 759 nm) and 11 from copper. With high-reflectivity visible mirrors, the Zn^+ transitions at 491, 492, 589, and 610 nm were also readily inverted in this brass cathode. We also experimented with a stainless steel hollow cathode and obtained anomalous laser action at 9 wavelengths: 703.5, 712.5, 719.9, 760.5, 770.9, 774.0, 775.3, 779.8, and 783.9 ± 0.5 nm. Inversion was obtained only in a helium discharge with $\sim 0.5\%$ addition of hydrogen. The first two of these lines were fairly strong, their thresholds being 7.5 and 6.3 A, respectively, and a peak quasi-cw output power of 50 mW was measured from these transitions with the 25 cm long slotted cathode at a discharge current of 20 A. In order to identify the laser lines, we examined the major constituents of type 304 stainless steel alloy [21]; iron (66.3% min), chromium (18–20%) and nickel (8–10.5%). None of the above lines was observed in our previous studies with chromium [10d] and nickel [10b] hollow cathodes. In an Fe cathode made from high-purity electron-beam melted iron flake, no stimulated emission was observed at all. Thus, we are unable to identify any of the above observed transitions.

In summary, operating characteristics of several hollow-cathode metal-ion lasers have been presented. Variation of the output power, gain and threshold current is studied as a function of the cathode length, output mirror coupling and buffer gas composition.

Acknowledgements. The authors would like to thank M. Klein, D. Schwartz, and J. Tracy for assistance.

References

1. E.K.Karabut, V.S.Mikhalevskii, V.F.Papakin, M.F.Sem: Sov. Phys. Tech. Phys. **14**, 1447–1448 (1970)
2. W.K.Schuebel: IEEE J. QE-**6**, 574–575 (1970)
3. Y.Sugawara, Y.Tokiwa: Jpn. J. Appl. Phys. **9**, 588–589 (1970)
4. (a) J.A.Piper, C.E.Webb: J. Phys. D (Appl. Phys.) **6**, 400–407 (1973);
   (b) J.A.Piper, P.Gill: J. Phys. D (Appl. Phys.) **8**, 127–134 (1975);
   (c) J.A.Piper, I.M.Littlewood, C.E.Webb: J. Phys. B (Atom. Mol. Phys.) **11**, 3731–3744 (1978)
5. L.Csillag, M.Janossy, K.Rozsa, T.Salamon: Phys. Lett. **50** A, 13–14 (1974)
6. K.Fujii, T.Takahashi, Y.Asami: IEEE J. QE-**11**, 111–114 (1975)
7. (a) J.R.McNeil, G.J.Collins, K.B.Persson, D.L.Franzen: Appl. Phys. Lett. **27**, 595–598 (1975);
   (b) J.R.McNeil, R.D.Reid, D.C.Gerstenberger, G.J.Collins: In *High-Power Lasers and Applications*, ed. by K.L.Kompa and H.Walther (Springer, Berlin, Heidelberg, New York, 1978) pp. 89–95;
   (c) B.E.Warner, D.C.Gerstenberger, R.D.Reid, J.R.McNeil, R.Solanki, K.B.Persson, G.J.Collins: IEEE J. QE-**14**, 568–570 (1978)
8. K.U.Baron, B.Stadler: Opt. Commun. **18**, 160–162 (1976)
9. N.V.Subotinov, J.Konieczka, J.Mizeraczyk, N.K.Vuchkov: Sov. J. Quantum Electron. **8**, 918–919 (1978)

10. K.Jain: (a) Appl. Phys. Lett. **34**, 398–399 (1979); (b) **34**, 845–846 (1979); (c) **36**, 10–11 (1980); (d) **37**, 362–364 (1980)
11. (a) H.J.Eichler, H.Koch, J.Pfaffenholz, J.Salk, Ch. Skrobol: J. Phys. (Paris) **40**, C7-379-380 (1979);
(b) H.J.Eichler, W.Wittwer: J. Appl. Phys. **51**, 80–83 (1980);
(c) H.J.Eichler, H.Koch, J.Salk, Ch. Skrobol: Opt. Commun. **34**, 228–230 (1980)
12. V.V.Vainer, S.P.Zinchenko, I.G.Ivanov, M.F.Sem: Sov. J. Quantum Electron. **10**, 581–586 (1980)
13. K.Gnadig, L.Fu-Cheng: Opt. Commun. **34**, 218–220 (1980)
14. J.R.McNeil, G.J.Collins, F.J.de Hoog: J. Appl. Phys. **50**, 6183–6189 (1979)
15. W.W.Rigrod: J. Appl. Phys. **34**, 2602–2609 (1963)
16. This is the shortest hollow-cathode ultraviolet laser demonstrated to date. In the ir, we were able to invert the 781 nm line from CuII in a 5 mm long cathode
17. J.R.McNeil: Ph.D. Thesis, Colorado State University, Fort Collins, CO (1977) (unpublished)
18. F.J.de Hoog, J.R.McNeil, G.J.Collins: J. Appl. Phys. **48**, 3701–3704 (1977)
19. B.E.Warner, K.B.Persson, G.J.Collins: J. Appl. Phys. **50**, 5694–5703 (1979)
20. See, for example, G.Carter, J.S.Colligan: *Ion Bombardment of Solids*. (American Elsevier, New York 1968)
21. *Marks' Standard Handbook for Mechanical Engineers*. 8th. ed., ed. by T. Baumeister, E.A.Avallone, T.Baumeister III (McGraw-Hill, New York 1978) pp. 6–37.